A secreted protease-like protein in *Zymoseptoria tritici* is responsible for avirulence on *Stb9* resistance gene in wheat

Reda AMEZROU[1], Colette AUDÉON[1], Jérôme COMPAIN[2], Sandrine GÉLISSE[1], Aurélie DUCASSE[1], Cyrille SAINTENAC[3], Nicolas LAPALU[1,2], Simon ORFORD[4], Daniel CROLL[5], Joëlle AMSELEM[2], Sabine FILLINGER[1], Thierry C MARCEL[1*]

[1] Université Paris-Saclay, INRAE, UR BIOGER, 91120 Palaiseau, France.
[2] Université Paris-Saclay, INRAE, UR URGI, 78026 Versailles, France.
[3] UCA, INRAE, GDEC, 63000 Clermont-Ferrand, France.
[4] Crop Genetics, John Innes Centre, Norwich NR4 7UH, UK.
[5] University of Neuchâtel, Laboratory of Evolutionary Genetics, 2000 Neuchâtel, Switzerland.

[*] Corresponding authors: thierry.marcel@inrae.fr; reda.amezrou@inrae.fr

Running title: The avirulence factor *AvrStb9* from *Zymoseptoria tritici*

Key words: Avirulence, Gene-for-gene interaction, Protease, GWAS, Wheat, *Zymoseptoria tritici*

Word count (main text): 6,141

Abstract

Zymoseptoria tritici is the fungal pathogen responsible for Septoria tritici blotch on wheat. Disease outcome in this pathosystem is partly determined by isolate-specific resistance, where wheat resistance genes recognize specific fungal factors triggering an immune response. Despite the large number of known wheat resistance genes, fungal molecular determinants involved in such cultivar-specific resistance remain largely unknown. We identified the avirulence factor *AvrStb9* using association mapping and functional validation approaches. Pathotyping *AvrStb9* transgenic strains on *Stb9* cultivars, near isogenic lines and wheat mapping populations, showed that *AvrStb9* interacts with *Stb9* resistance gene, triggering a strong immune response. *AvrStb9* encodes an unusually large avirulence gene with a predicted secretion signal and a protease domain. It belongs to a S41 protease family conserved across different filamentous fungi in the Ascomycota class and may constitute a core effector. *AvrStb9* is also conserved among a global *Z. tritici* population and carries multiple amino acid substitutions caused by strong positive diversifying selection. These results demonstrate the contribution of an 'atypical' conserved effector protein to fungal avirulence and the role of sequence diversification in the escape of host recognition, adding to our understanding of host-pathogen interactions and the evolutionary processes underlying pathogen adaptation.

Author Summary

Fungal avirulence (Avr) genes are involved in gene-for-gene relationships with host resistance genes. Avr genes may at the same time target host defenses to allow infection and be recognized by a host resistance gene triggering a defense response. It is commonly assumed that most Avr genes encode small secreted proteins, with no predicted functional domain and no sequence homology in other species. But the use of methods without *a priori* on the function or structure of genetic determinants may allow to identify Avr genes coding for proteins not falling into this category. Following a genome-wide association (GWA) approach in *Zymoseptoria tritici*, an important wheat fungal pathogen causing the Septoria tritici blotch disease, we could identify and clone *AvrStb9*, an unusually large Avr gene with a predicted secretion signal. AvrStb9 belongs to a family of proteins with a predicted protease S41 domain conserved across diverse ascomycete lineages. The recognition of *AvrStb9* by hosts carrying *Stb9* resistance gene triggers a strong immune response following the gene-for-gene model.

Introduction

Filamentous fungal pathogens are responsible for the most damaging crop diseases [1]. Their ability to cause disease is facilitated by fungal proteins called effectors, which are delivered into the plant apoplast or cytoplasm during the infection process [2,3]. Effectors play critical role in the infection by manipulating plant immune system and other cellular functions. To counteract fungal infections, plants have evolved efficient defense systems relying on the recognition of different fungal factors [4]. The first type of defense involves plant receptors recognizing generic fungal molecules, called pathogen-associated molecular patterns (PAMPs). This PAMP-triggered immunity (PTI) provides basal defense against non-adapted pathogens. The second type of defense is activated with the recognition of fungal effectors by plant receptors, defined as resistance (*R*) genes. Effector-triggered immunity (ETI) induces a specific and strong immune response thought to limit the infection [4]. This interaction typically follows the gene-for-gene model, where host *R* gene products recognize pathogen effectors, which are then called avirulence (*Avr*) genes [5]. However, ETI exerts a strong evolutionary pressure on pathogen populations leading to the selection of virulent isolates overcoming host immune response [2]. Most of these virulent isolates displayed mutations in the avirulence gene leading to variant proteins not recognized by the corresponding R protein [6]. These observations emphasize the importance of pathogen *Avr* genes surveillance and the adequate spatiotemporal deployment of *R* genes in the field.

A common assumption is that most *Avr* genes encode small secreted proteins (SSP), with no predicted functional domain and no sequence homology in other species [7,8]. It is often overlooked that *Avr* genes may also code for proteins not strictly falling into this category. For instance, some *Avr* genes from *Cladosporium fulvum* (*Avr2* and *Avr4*), *Magnaporthe oryzae* (*Avr-Pita*) or *Melampsora lini* (*AvrM14*) encode proteins that share sequence similarities with known enzymes or enzyme inhibitors (reviewed in [8]). However, only few such 'atypical' avirulence factors have been described in literature

so far and their identification will broaden our knowledge on the complex molecular cross-talk between plants and pathogens.

Zymoseptoria tritici is an ascomycete fungal pathogen that causes the major wheat foliar disease Septoria tritici blotch (STB). *Z. tritici* is apoplastic with a biphasic infection process [9]. After penetration into wheat leaves through stomata, the fungus colonizes the apoplast for 8-11 days while the host remains symptomless [10]. This long asymptomatic phase is followed by a rapid onset of necrotic symptoms, associated with the development of fungal asexual fruiting bodies called pycnidia, which contain the pycnidiospores that further spread the disease [11]. STB is currently the economically most important wheat disease in Europe and is mainly controlled using fungicides and genetic resistances [9,12]. However, this disease remains a problem due to the ability of fungal populations to overcome control measures (*i.e.*, fungicide resistance, host resistance breakdown) and adapt to climate changes [12]. Despite its economic importance, the molecular basis of *Z. tritici* avirulence remains largely unknown. Only two avirulence genes have been characterized so far, *AvrStb6*, recognized by the resistance protein *Stb6* leading to a strong immune response; and *Avr3D1* which is thought to trigger quantitative resistance in cultivars carrying *Stb7* resistance gene [13,14,15]. Both genes encode SSPs located in highly plastic genomic regions rich in transposable elements thought to favor their rapid diversification [13,15]. In addition to *Stb6* and *Stb7*, 21 major isolate-specific STB resistance genes have been mapped in wheat, but their corresponding avirulence genes remain unknown [16,17,18].

Here, we aimed to broaden our understanding of avirulence in fungal pathogens, the mechanisms underlying gene-for-gene interactions in the *Z. tritici*–wheat pathosystem and the evolutionary processes related to the escape of host recognition. We first showed that a large protein encoding a predicted secreted protease, *AvrStb9*, is responsible for avirulence in a subset of fungal strains. We demonstrated that recognition *AvrStb9* by hosts carrying *Stb9* resistance gene triggers a strong immune response following the gene-for-gene model. We next showed that *AvrStb9* belongs to a family of proteins with a predicted protease S41 domain conserved across diverse ascomycete lineages and that mutations in *AvrStb9*, including some in the predicted protease domain, led to variants escaping *Stb9*-mediated recognition.

Results

Mapping of a candidate gene conferring avirulence on the cultivar 'Soissons'.

'Soissons' is a French bread wheat variety, developed by Florimond Desprez and released in 1987, which represented 10 to 40% of the French wheat acreage between 1991 and 2002. 'Soissons' is moderately susceptible to STB [19] but it has been postulated to carry the resistance gene *Stb9* based on screening with differentially virulent isolates (data not shown). Infection assays of the fungal population on cultivar 'Soissons' showed that ~12% of the French isolates are avirulent (Fig. S1). We conducted GWAS to identify the *Avr* gene interacting with the resistance in 'Soissons'.

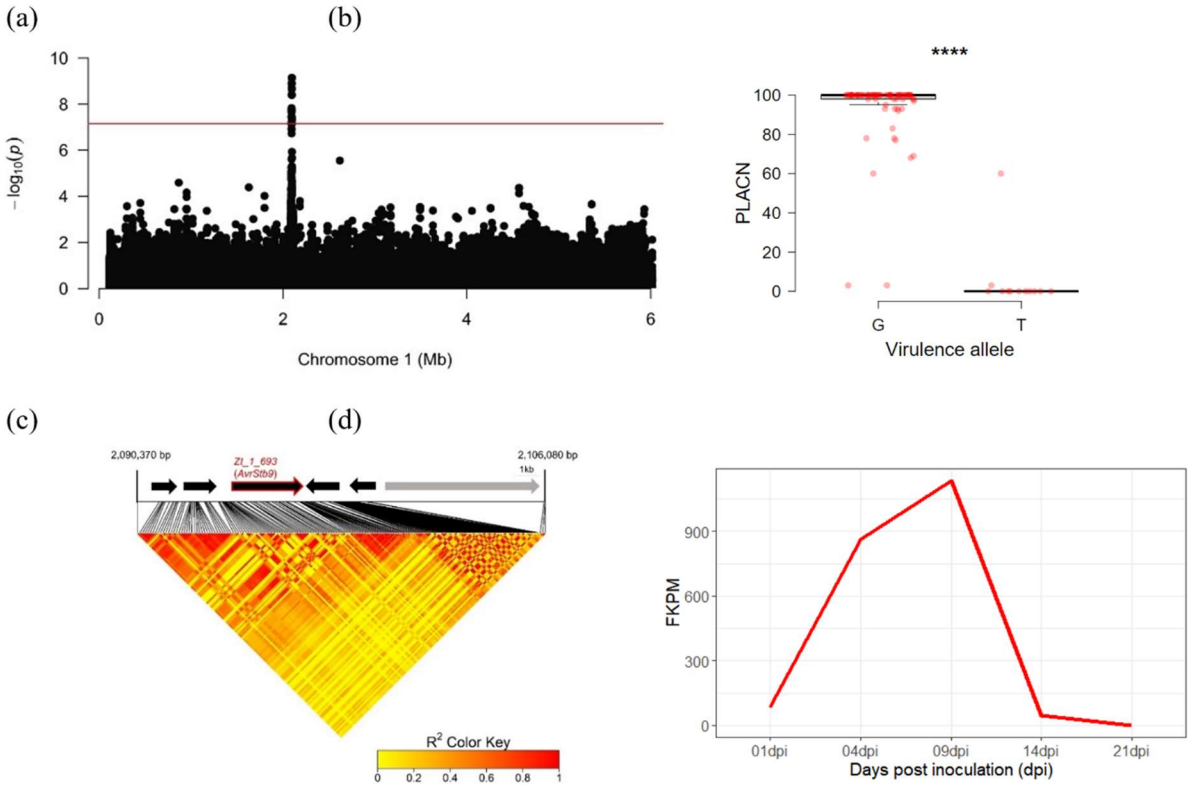

Figure 1. GWAS identifies a candidate gene controlling avirulence on the cultivar 'Soissons'. (a) Manhattan plot representing the association of multiple SNPs with PLACN on cultivar 'Soissons'. The X and Y axes indicate positions on chromosome 1 and −log10 (*p*-value) for associations, while the red line represents the Bonferroni threshold (α=0.05). (b) Top: Gene annotations (black arrows) and transposable elements (grey arrow) on the reference genome IPO323. The candidate gene is highlighted in red. Bottom: Pairwise linkage disequilibrium plot around the lead significant SNP. The association peak is associated with several polymorphisms in the gene *Zt_1_693*. (c) The difference in PLACN of isolates carrying the virulent and avirulent alleles (based on the lead SNP). Significance difference from the mean was computed using a two-sided Mann-Whitney test (****, $p<0.0001$). (d) Gene expression profile of *Zt_1_693* measured as fragments per kilobase of exon per million mapped fragments (FPKM) throughout the time course of *Z. tritici* infection on a susceptible wheat cultivar [20].

A total of 103 *Z. tritici* strains were re-sequenced, generating 718,810 SNPs passing quality filters. Using full SNP data, we investigated the population structure and kinship and found very little genetic substructure and relatedness in the fungal population (Fig. S2a,b). For instance, the first three PCs accounted for only 3.11% of the total genetic variation. Using a linear mixed model to associate genetic variations with pycnidia (PLACP) and necrosis (PLACN) variations on 'Soissons', we identified a cluster of 26 SNPs on chromosome 1 from 2,092,563 bp to 2,096,143 bp, significantly associated with PLACN at the Bonferroni threshold (Fig. 1a). The same SNP cluster was also associated with variation in PLACP but failed to reach the genome-wide significance (Fig. S3). We also detected a significant association with PLACN variations (p=3.801e-8; position 2,451,010 bp) on a segment of chromosome 7. However, the region falls in a broad section of the chromosome without any *in planta* expressed genes

130 [20]. The significant SNPs on chromosome 1 mapped to a region containing two predicted genes,
131 *Zt_1_692* and *Zt_1_693*. The lead SNP (*p*=7.31e-10; position 2,095,552 bp) mapped to the fourth exon
132 of *Zt_1_693*, but was in strong linkage disequilibrium with other variants spanned across the two
133 predicted genes (Fig. 1b). *Zt_1_692* is not expressed *in planta* so we were unable to use RNA-seq data
134 to evaluate the quality of the gene annotation and blastp searches yielded only weak hits. Without any
135 corroborating evidence for a biological role, we concluded that *Zt_1_692* is likely a pseudogene or an
136 annotation error. In contrast, *Zt_1_693* is highly expressed *in planta* (Fig. S4), with a peak expression
137 at 9 days post infection coinciding with the switch from asymptomatic to necrotrophic phase (Fig. 1d).
138 Further, allele analyses of the lead SNP clearly discriminated between avirulent and virulent phenotypes
139 (Fig. 1c). Taken together, we considered *Zt_1_693* as the best candidate gene to explain avirulence on
140 the wheat cultivar 'Soissons'.

141 ***Zt_1_693* is involved in a gene-for-gene relationship with *Stb9* resistance gene.**

142 To determine whether *Zt_1_693* is an avirulence factor recognized by an *R* gene in the cultivar
143 'Soissons', we sought to generate *Zt_1_693* deletion mutants (KO) in the virulent strain IPO323 and
144 four different avirulent strains by targeted gene replacement. We also switched alleles between avirulent
145 (IPO09395) and virulent (IPO323) strains using targeted gene replacement. However, we could not
146 obtain any deletion mutant neither in IPO323 (144 transformants tested), nor in the avirulent strains
147 IPO09593, IPO09359 and IPO09139 (n=95). Only a single deletion mutant was obtained in strain
148 SYN32 out of 32 transformants, producing small colonies and weak symptoms on the susceptible
149 cultivar 'Taichung-29' (Table S3). This suggests that *Zt_1_693* could be essential for *Z. tritici* growth,
150 and pathogenicity. Nevertheless, using allele swapping we were able to generate mutants expressing the
151 virulent and avirulent versions of *Zt_1_693* in IPO323 genetic background, and performed infection
152 assays on cultivars 'Soissons', 'Courtot' which carries the *Stb9* gene and a 'Courtot' near isogenic line
153 lacking *Stb9*.

154 IPO323 gene replacement transformants carrying the avirulent allele (n=6) from IPO09593 (referred to
155 as *Avrstb9*) were avirulent on 'Soissons' and 'Courtot', but not on 'Courtot' lacking *Stb9* (Fig. 2a).
156 Inversely, gene replacement transformants with the virulent allele (referred to as *avrstb9*) from IPO323
157 (n=2) resulted in virulence on all tested cultivars, with PLACP values at 26 dpi ranging from 32 to 100%
158 (Fig. 2a). Interestingly, Sanger sequencing of $IPO323_{Avrstb9}$ transformants revealed that four strains were
159 chimeric with the avirulent allele not being introduced in full length, retaining some polymorphisms of
160 the virulent haplotype between residues 276 and 628. All four chimeric strains were virulent on *Stb9*-
161 containing cultivars, highlighting the importance of these polymorphisms in virulence (Table 1; Table
162 S3; Fig. S6). The fact that all IPO323 mutants carrying the complete *AvrStb9* allele were unable to infect
163 *Stb9*-containing cultivars, while mutants expressing the *avrStb9* allele produced symptoms on all three

cultivars, suggest that *Zt_1_693* encodes the avirulence factor *AvrStb9*, which triggers complete resistance in cultivars carrying the cognate resistance gene.

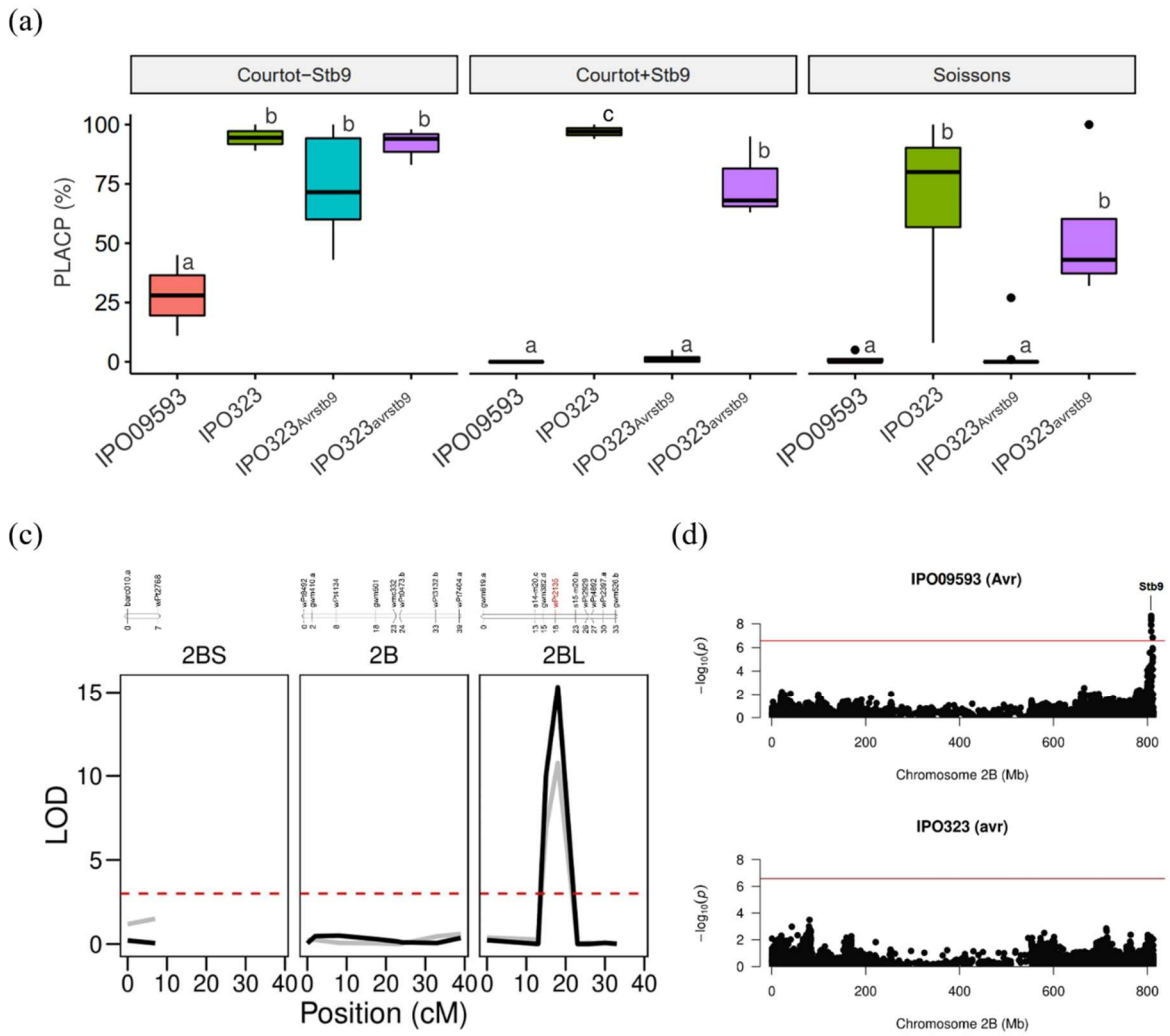

Figure 2. *Zt_1_693* encodes for the avirulence gene *AvrStb9* and triggers *Stb9* resistance. (a) PLACP at 26 dpi measured after inoculation with the avirulent isolate IPO09593, the virulent isolate IPO323 and IPO323 mutants expressing the avirulent allele (IPO323$_{Avrstb9}$) or the virulent allele (IPO323$_{avrstb9}$) on cultivars 'Courtot' (*Stb9*), a 'Courtot' mutant lacking *Stb9* and 'Soissons' (details on the phenotype of each mutant is provided in Fig. S6; Table S6). Statistical significance was determined using a Tukey's HSD test. (b) Genetic mapping of *Stb9* resistance gene using linkage mapping. Top panel: Linkage map and marker position in cM. Bottom panel: Logarithm of odds (LOD) score plot of the QTL analysis (Relative AUDPC for sporulation and necrosis in black and grey, respectively) possibly containing the *Stb9* locus mapped to the long arm of the chromosome 2B. The horizontal dashed line indicates a suggestive linkage threshold (LOD = 3). The position of the marker in the QTL peak is highlighted in red. (c) Manhattan plots representing association mapping results of relative AUDPC sporulation of the avirulent (top) and virulent (bottom) isolates in the bread wheat panel. Multiple SNPs in the telomeric region of chromosome 2B associated with the avirulent isolate are located in the *Stb9* genomic region.

Table 1. Polymorphisms in AvrStb9 protein sequences between the wild type and transgenic mutant strains. Difference in amino acid residues between the virulent (avrstb9) and avirulent (Avrstb9) phenotypes are highlighted in orange while residues potentially involved in virulence are highlighted in red.

Strain	**Mutant ID**	**Codon position / Amino acid residue**													**Phenotype (on *Stb9*)**
		58	**66-71**	**73**	**188**	**276**	**349**	**370**	**431**	**473**	**512**	**525**	**565**	**628**	
Wild-type strains															
IPO323 (avrstb9)	-	R	PCNSTI	N	Y	T	A	T	A	F	S	S	D	L	Virulent
IPO09593 (Avrstb9)	-	Q	Δ	D	V	N	V	N	D	Y	T	F	N	Y	Avirulent
IPO323 Avrstb9 transformants															
IPO323$_{Avrstb9}$ hph#5	E	Q	Δ	D	V	N	V	N	D	Y	T	F	N	Y	Avirulent
IPO323$_{Avrstb9}$ hph#6	F	Q	Δ	D	V	N	V	N	D	Y	T	F	N	Y	Avirulent
IPO323$_{Avrstb9}$ hph#9	H	Q	Δ	D	V	N	V	N	D	Y	T	F	N	Y	Avirulent
IPO323$_{Avrstb9}$ hph#12	K	Q	Δ	D	V	N	V	N	D	Y	T	F	N	Y	Avirulent
IPO323$_{Avrstb9}$ hph#14	L	Q	Δ	D	V	N	V	N	D	Y	T	F	N	Y	Avirulent
IPO323$_{Avrstb9}$ hph#18	N	Q	Δ	D	V	N	V	N	D	Y	T	F	N	Y	Avirulent
IPO323 Avrstb9 chimeric transformants															
IPO323$_{Avrstb9}$ hph#3	I	Q	Δ	D	V	T	A	T	A	F	S	S	D	L	Virulent
IPO323$_{Avrstb9}$ hph#11	J	Q	Δ	D	Y	T	A	T	A	F	S	S	D	L	Virulent
IPO323$_{Avrstb9}$ hph#7	G	Q	Δ	D	Y	T	A	T	A	F	S	S	D	L	Virulent
IPO323$_{Avrstb9}$ hph#17	M	Q	Δ	D	V	N	A	T	A	F	S	S	D	L	Virulent
IPO323 avrstb9 transformants															
IPO323$_{avrstb9}$ hph#3	O	R	PCNSTI	N	Y	T	A	T	A	F	S	S	D	L	Virulent
IPO323$_{avrstb9}$ hph#4	P	R	PCNSTI	N	Y	T	A	T	A	F	S	S	D	L	Virulent
Percentage of virulent isolates in the fungal population		87.5	98.86	86.63	98.86	98.86	54.54	88.63	**98.86**	**98.86**	89.77	**98.86**	**98.86**	**95.54**	
Probability of dN/dS>1		0.97	-	0.99	0.99	0.58	0.54	0.59	0.93	0.60	**0.99**	**1.00**	0.65	**1.00**	

183 To further validate the *AvrStb9-Stb9* gene-for-gene relationship, we performed two independent genetic
184 analyses using a bi-parental mapping population and a panel of wheat varieties. The isolate-specific
185 resistance to IPO09593 (*AvrStb9*) was mapped by a QTL analysis on Beaver/Soissons recombinant
186 double haploid progenies. A single major resistance QTL was detected on the long arm of the wheat
187 chromosome 2B, likely corresponding to the *Stb9* locus [21]. This QTL had a log-likelihood (LOD) of
188 10.77 and 15.33 for the RAUDPC of necrosis and sporulation, respectively (Fig. 2b). As expected, the
189 resistance allele originated from 'Soissons' suggesting that the cultivar indeed carries the *Stb9*
190 resistance. We confirmed this interaction by performing a GWAS analysis on a wheat panel phenotyped
191 using the virulent and avirulent strains. Association mapping results revealed a strong signal associated
192 with RAUDPCs for the avirulent strain IPO09593 (eight SNPs above the Bonferroni-corrected cutoff)
193 in the telomeric region of chromosome 2B, but not with the virulent strain IPO323 (Fig. 2c). This
194 confirms that IPO09593 triggers a strong resistance from varieties carrying a resistance QTL in the
195 vicinity of the *Stb9* gene. Additional details on *Stb9*-associated SNPs are provided in the supplemental
196 Table S1. Finally, based on the lead SNP (AX-89505650; position 808,036,267 bp on chromosome 2B),
197 phenotypic and allele analyses showed that ca. 8.2% of the French varieties likely carry *Stb9*.

198 Altogether, our combined functional and genetic analyses demonstrate that *Zt_1_693* is the avirulence
199 gene *AvrStb9* and is involved in a gene-for-gene relationship with *Stb9* resistance in wheat.

200 ***AvrStb9* encodes a secreted protein with a conserved protease domain shared among diverse**
201 **ascomycete lineages.**

202 Unlike other known fungal effectors, *AvrStb9* encodes a large protein and shares sequence similarities
203 with different fungal species. The re-annotated *AvrStb9* gene model has five introns and encodes a 727
204 amino acid long protein with eight cysteine residues (Fig. 3a; 3b). This protein has a predicted signal
205 peptide sequence of 18 amino acids at its N-terminus and two serine-protease domains (C-terminal
206 processing peptidase S41 family; positions 70-726; Fig. 3b) according to InterProScan (Panther entry
207 PTHR-37049, e-value: 2.7 e-64). HHpred searches in protein structure databases identified the secreted
208 protease CPAF as the strongest hit (e-value of 1.5e-27), which is involved in pathogenesis of the human
209 pathogenic bacterium *Chlamydia trachomatis* [22].

210 To investigate whether *AvrStb9* originated before or after *Z. tritici* speciation, we used blastp searches
211 against *Z. tritci* reference genome IPO323 and closely-related species from the *Zymoseptoria* family.
212 We identified *AvrStb9* and its paralogs from IPO323 and all its closest relatives *Z. pseudotritici, Z.*
213 *ardabiliae* and *Z. brevis* (Fig. S7a). Interestingly, most of these proteins had a predicted signal peptide,
214 and they all displayed a C-terminal processing peptidase S41 domain. Using IPO323 *in planta* gene
215 expression, we found that three out of the five paralogs (*Zt_4_489, Zt_10_226, Zt_11_236*) had an
216 expression profile comparable to *AvrStb9* (Fig. S7b). According to these expression patterns, these genes
217 could potentially play a role in infection.

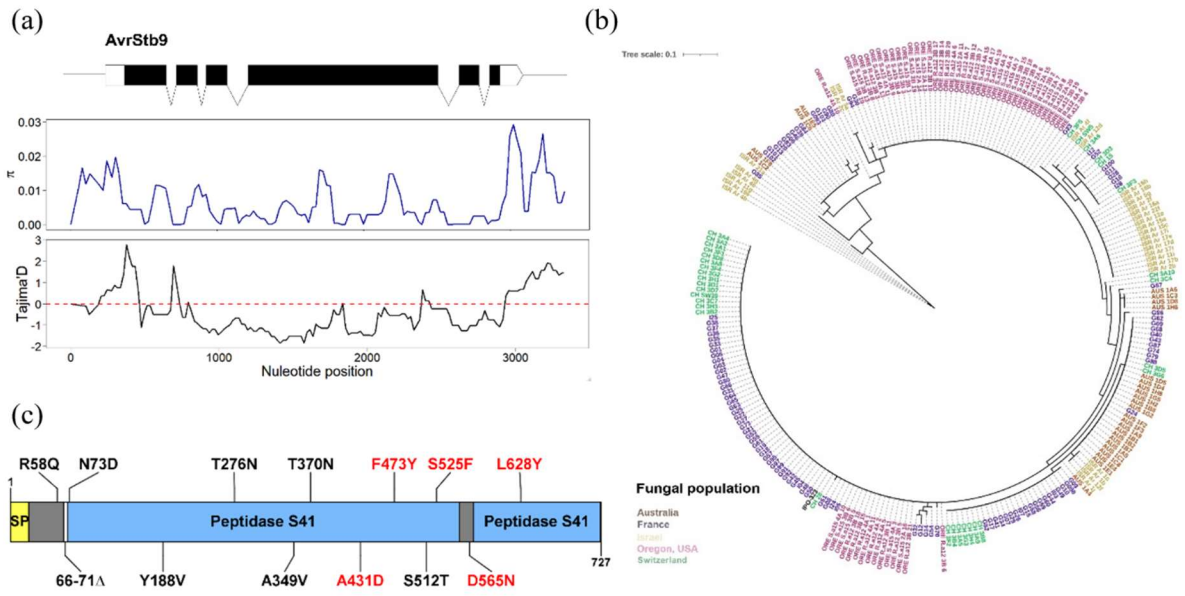

Figure 3. *AvrStb9* diversity and phylogeny in the global *Z. tritici* population. (a) The top panel shows the *AvrStb9* gene structure. Middle and low panels are sliding window analyses for nucleotide diversity (π) and Tajima's D across the *AvrStb9* locus, respectively, with a window size of 200 bp and a step size of 20 bp. The plots show a reduced nucleotide diversity and a drop in Tajima's D values, likely corresponding to a selective sweep spanning the region. (b) Schematic diagram of *AvrStb9* protein sequence with an annotation of amino acid substitutions between virulent and avirulent alleles. Substitutions potentially involved in virulence are highlighted in red. SP=Signal peptide. (c) A phylogenetic tree of *AvrStb9* protein sequence generated from a global *Z. tritici* population and the reference isolate IPO323.

Using OrthoMCL, we identified 122 putative *AvrStb9* orthologs/paralogs with an average identity of 33.6% and an average e-value of 8e-73 (Table S4). *AvrStb9* orthologs/paralogs are found in a broad range of ascomycete lineages belonging to Eurotiomycetes, Leotiomycetes, Sordariomycetes, Orbiliomycetes and Dothideomycetes (Fig. 4; Table S4). Most of fungal species (48 out of 65 species) identified from the orthogroup are pathogenic, indicating that the well conserved *AvrStb9* orthologs/paralogs may be involved in host interaction processes. Interestingly, ~87% of these proteases possess a predicted signal peptide.

Diversification of *AvrStb9* leads to evasion of host recognition

Non-synonymous substitutions in avirulence gene sequences often mediate the evasion of host recognition. Analysis of sequence polymorphisms between the avirulent and virulent strains revealed a 6 amino acid deletion and 12 non-synonymous substitutions (Table 1; Fig. 3b). We crossed this data with the fungal population phenotypes and identified eight mutations potentially involved in host evasion for which more than ~94% of strains carrying the mutation were virulent on *Stb9* cultivars (Table 1). Five of these mutations fall into the virulence-domain cited above, namely A431, F473, S525, D565, L628. All of these mutations except D565 are located in one of the two putative protease domains

(Fig. 3b), with F473, S525 and L628 being relatively conserved residues among proteins belonging to the CPAF structural family (in 34-57% of the analyzed proteins respectively; data not shown).

In order to investigate *AvrStb9* diversity at a larger scale, we extended our analysis to include four global *Z. tritici* populations. We found 44 different *AvrStb9* alleles in these populations, which translate to 38 different protein variants, mostly population-specific (Fig. 3c). Next, we analyzed *AvrStb9* nucleotide diversity including ~500 bp of up- and downstream sequences from the start and stop codons, respectively. We observed both a drop-in nucleotide diversity and Tajima's D in the *Avr* coding sequence compared to the flanking regions (Fig. 3a). A negative Tajima's D is indicative of an excess of low frequency polymorphisms, indicating population size expansion and/or selective sweeps.

The codon-based model analysis of *AvrStb9* coding sequence was used to investigate the selection pressure exerted on the avirulence gene. Likelihood ratio tests (LRT) for different models indicated that positive selection was highly probable, as selection models (M2 and M8) showed a significantly better data fit compared to the neutral models M1 and M7 (Table S5). Selection analysis revealed 23 residues (3.16% of the protein sequence) under positive diversifying selection (BEB probability > 0.95) in the M2 model. Interestingly, S525F and L628Y, had the strongest positive selection probability (BEB probability of = 1) among the five mutations potentially responsible of the virulence according to the previous analyses (Table 1). We postulate that these adaptive mutations are under strong selective pressure most probably to counteract recognition by the *Stb9* resistance gene.

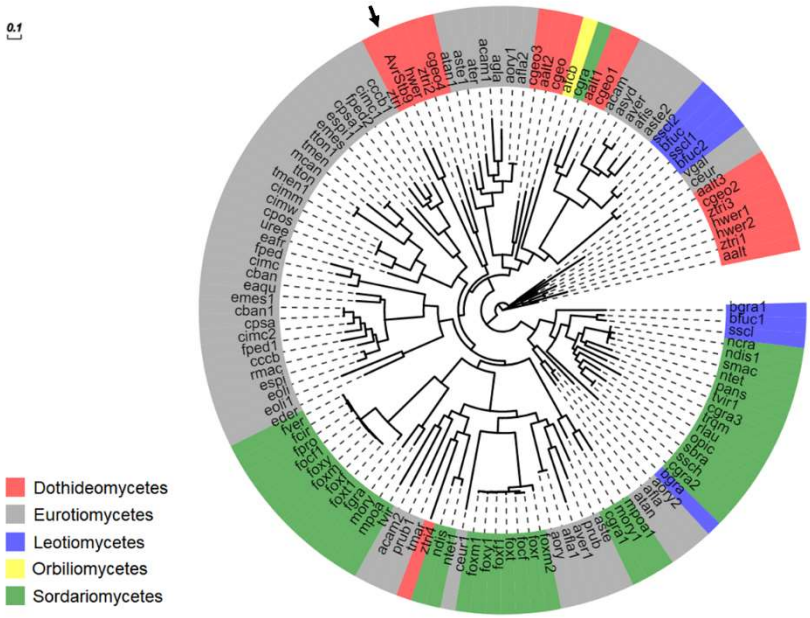

Figure 4. Phylogenetic tree of selected *AvrStb9* orthologs/paralogs belonging to five distinct classes of Ascomycota lineages. Leaf labels are color-coded according to class and represent abbreviated names of the fungal species (Table S4). *AvrStb9* is indicated with a black arrow.

264 **Discussion**

265 Gene-for-gene interactions in plant pathosystems are described when a host resistance gene recognizes
266 a pathogen's avirulence product that triggers a strong host immune response. Although 23 isolate-
267 specific *Stb* resistance genes have been mapped in wheat, only two have been cloned so far and their
268 corresponding fungal avirulence genes remain largely unknown. Here, we report the identification and
269 characterization of a novel avirulence gene, *AvrStb9*, which triggers complete resistance in wheat
270 cultivars carrying *Stb9* resistance gene. Additionally, we performed a high-resolution mapping of *Stb9*
271 locus and delivered tightly-linked SNP markers for its use in breeding.

272 *AvrStb9* is highly expressed during the asymptomatic phase of *Z. tritici* infection and drastically
273 downregulated upon the switch to the late necrotrophic phase. In a previous study, *AvrStb9* was among
274 the top 100 highly expressed genes during the transition from biotroph to necrotrophy stage [23],
275 suggesting a function in host colonization during the asymptomatic phase or the transition to the
276 necrotrophic phase. Recognition of the *Avr* allele leads to full resistance in cultivars carrying *Stb9*
277 following the gene-for-gene model. A previous study mapped the *Stb9* resistance locus to the long arm
278 of chromosome 2B but the genomic interval remained very large [21]. We used *AvrStb9* strain to trigger
279 wheat resistance and perform a precise mapping of the resistance locus, which revealed that *Stb9* resides
280 in the telomeric region of wheat chromosome 2B in an interval of 79.99-81.10Mb ($r^2 > 0.50$). Only two
281 STB resistance genes have been cloned to date, *Stb6* and *Stb16q*, both encoding receptor-like kinase
282 proteins [24,25], and our findings will help in the cloning of *Stb9* resistance gene.

283 *AvrStb9* is an atypical fungal avirulence gene, since it encodes a relatively large secreted protein (727
284 aa). Up to now, avirulence genes from filamentous fungal pathogens encode small (< 300 aa) secreted
285 proteins rich in cysteine. Only three exceptions to this rule are the *Ace1* gene from *Magnaporthe grisea*
286 [26] encoding a large polyketide synthase (PKS) fused to a nonribosomal peptide synthetase (NRPS)
287 likely involved in secondary metabolism, and two *AvrMla* genes from *Blumeria graminis hordei* which
288 encode large proteins [27]. Furthermore, in contrast to what has been shown for most avirulence genes,
289 *AvrStb9* has a predicted functional domain corresponding to the family of C-terminal processing S41
290 proteases and show sequence similarities with proteins from diverse fungal species. In plant pathogenic
291 bacteria, some type III secreted effectors injected in host plant cells are similar to catalytic enzymes
292 involved in a variety of reactions such as E3 ligation or proteolysis [28]. For instance, *Pseudomonas*
293 *syringae* secretes the cysteine protease *HopN1* to suppress the host innate response and promote
294 virulence [29].

295 The importance of proteases in fungal pathogenicity has previously been reported [30,31]. *Fusarium*
296 *oxysporum* f. sp. *lycopersicum* secretes a serine protease and a metalloprotease that cleave host
297 chitinases to prevent the degradation of fungal cell walls and facilitate host colonization [32]. The maize
298 anthracnose fungus *Colletotrichum graminicola* secretes a highly conserved metalloprotease effector

299 that enhances virulence [33]. Similarly, the rice blast fungus *Magnaporthe oryaze* secretes during
300 infection *Avr-Pita*, an effector protein with a predicted zinc metalloproteases domain that belongs to a
301 family of proteases that include other avirulence genes recognized by the resistance gene *Pi-ta* [34,35].
302 Our protein analyses (OrthoMCL, InterProScan, HHpred) indicated that AvrStb9 has sequence and
303 structural features typical of a protease. Protein structure-based homology searches identified the
304 secreted protease CPAF from the human pathogenic bacterium *C. trachomatis* as closest homolog.
305 CPAF degrades host transcription factors and therefore directly helps *Chlamydia* evading the host
306 defenses. We postulate that AvrStb9 could play a similar role in proteolytic degradation of host protein
307 substrates. However, the enzymatic activity of AvrStb9 is yet to be investigated, as our analysis relied
308 primarily on sequence and structure comparisons. Further, the fact that we were hardly able to produce
309 *AvrStb9*-disrupted mutants indicates that the gene may play an important role in *Z. tritici* survival, and
310 that the proteolytic activity likely extends to include substrates essential for fungal growth.

311 The broad conservation of AvrStb9 in *Z. tritici* world population, its sister species and some other fungal
312 species suggested that this protein is a core effector shared among these lineages. Irieda *et al.* [36]
313 reported the conservation of *NIS1* effector that was initially detected from two *Colletotrichum* spp. in a
314 wide range of Ascomycota and Basidiomycota lineages. *NIS1* targets plant immune kinases to suppress
315 PAMP-triggered immunity [36]. We hypothesize that S41 proteases may have been anciently acquired
316 by fungi, and that the expansion of particular serine protease families is associated with the evolution of
317 fungal lifestyle. Indeed, S41 serine proteases are suspected to have a role in programmed cell death and
318 pathogenic life style adaptation in fungi [37]. We also identified multiple paralogs from multiple fungal
319 species, likely resulting from gene duplication events, highlighting either the redundancy of these genes
320 or their evolution to interact with different substrates. The functional redundancy of virulence genes has
321 been a technical challenge to study their biological functions, as disruption mutants often lead to the
322 conclusion that these genes are not essential for pathogenicity [38,39]. These redundancies may also
323 increase the organism's genetic robustness against null mutations or act in compensation of a gene loss
324 [40]. In *Z. tritici* for instance, the different *AvrStb9* paralogs had a secretion signal and show an
325 expression pattern consistent with a role as effectors. Taken altogether, we hypothesize that *AvrStb9* and
326 related S41 proteases constitute a set of core effectors gained early in the evolution of fungal-plant
327 interactions.

328 Recognition of effectors by host resistance exerts an evolutionary pressure that favors sequence
329 diversification, effector deletion or acquisition to counteract the immune response. We analyzed
330 AvrStb9 sequence diversity and found a broad conservation of its protein residues, unlike the other
331 known *Z. tritici* avirulence genes, *AvrStb6* and *Avr3D1i* [41,15]. Nevertheless, we identified few
332 substitutions undergoing strong positive diversifying selection. Additional data from chimeric AvrStb9
333 transformants, from *Z. tritici* populations and from sequence conservation among the CPAF family
334 indicate S525 and L628 as probably the most important residues involved in virulence, although

335 combinations of mutations may be necessary. Based on the structural model for CPAF function, one
336 may speculate that a functional protease is required to escape host recognition.

337 This is corroborated by the fact that, we did not observe in any of the global strains a loss of *AvrStb9* or
338 other deleterious mutations. Furthermore, *AvrStb9* deletion proved to be nearly impossible (only one
339 poorly growing transformant had the gene deletion out of the 271 tested). We therefore suggest that
340 *AvrStb9* plays an essential role in the biology of *Z. tritici*. It is tempting to speculate that the functional
341 AvrStb9 protein actively degrades (through proteolysis) both fungal protein(s) and host defense
342 protein(s). Additional functional studies, including mutating the S41 protease active sites in virulent and
343 avirulent alleles will shed light on the role of the protease activity of AvrStb9 in its diverse biological
344 activities (fungal growth, wheat infection, recognition by *Stb9*). But also, the function of the wheat
345 resistance factor Stb9 is intriguing. Does it work as classical receptor protein, recognizing the avirulent
346 AvrStb9 protein? Does it inhibit AvrStb9 protease activity or, on the contrary, may the Stb9 resistance
347 protein be the target of AvrStb9 protease?

348 In conclusion, we identified a new major avirulence factor of *Z. tritici* that triggers a strong immune
349 response in hosts carrying the corresponding resistance gene. Unlike what has been described for most
350 avirulence genes, *AvrStb9* encodes a large protein with a predicted protease domain and likely belongs
351 to a family of conserved fungal S41 proteases. This is an important step in deciphering molecular
352 mechanisms underlying wheat – *Z. tritici* interactions, and shed light on the role of 'atypical' effectors
353 (*i.e.*, non-SSPs) in fungal avirulence. It opens new research avenues to broaden our knowledge on host-
354 pathogen interactions, in particular the characterization of enzyme activity of effectors, which will
355 greatly help our understanding of the biology of protease effectors, commonly found in fungal
356 pathogens.

357

358 ## Materials and Methods

359 ### Fungal material

360 A total of 103 *Z. tritici* strains were used for GWAS analysis. The strains derive from a French *Z. tritici*
361 collection collected in 2009 on cultivars 'Apache' (n = 44), 'Premio' (n = 42), 'Soissons' (n = 9),
362 'Caphorn' (n = 3), 'Alixan' (n = 1), 'Bermude' (n = 1), 'Dinosaur' (n = 1) and 'Garcia' (n = 1); one
363 isolate was collected in the UK on cultivar 'Humbert'. The two isolates used for genetic mapping of the
364 resistance and fungal transformation are IPO323 and IPO09593. IPO323 is a Dutch isolate collected on
365 cultivar 'Arminda' in 1981 and used as the reference strain for *Z. tritici* [42]. IPO09593 is part of the
366 103 strains and has been isolated from 'Apache' in 2009. IPO323 is virulent on cultivars carrying *Stb9*
367 resistance gene while IPO09593 is avirulent on *Stb9*-cultivars. The three additional isolates used to
368 construct deletion and allele swap transformants, namely IPO09359 ('Apache', 2009), IPO09139
369 ('Apache', 2009) and SYN32 (unknown cultivar, 2006), are avirulent on *Stb9*-cultivars.

370 **Plant material**

371 We performed quantitative trait loci (QTL) mapping in a recombinant doubled haploid (DH) population
372 comprised of 65 lines, developed from the F_1 progeny of the cultivars 'Beaver' and 'Soissons' [43]. A
373 panel of 220 modern French bread wheat (BW) varieties was used for GWAS analysis; details on the
374 BW panel used here can be found in [44]. We also characterized *Z. tritici* wild-type and mutant strains
375 on near isogenic lines (NILs) carrying or not the *Stb9* resistance gene in the genetic background of
376 cultivar 'Courtot', developed at INRAE GDEC (Clermont-Ferrand, France). The 'Courtot' NILs were
377 developed following three backcrosses starting with F_1 'Courtot' x 'Chinese spring' (carrying a
378 susceptible allele of *Stb9* gene). To keep the *Stb9* susceptible allele in the progenies, each plant was
379 genotyped with single sequence repeat markers wmc317 and barc129 and phenotyped with the *Stb9*
380 avirulent isolate IPO89011. A BC_3F_1 plant heterozygous at the *Stb9* locus was self-fertilized. BC_3F_2
381 plants homozygous either for the susceptible *Stb9* allele ('Courtot' – Stb9) or for the resistant allele
382 ('Courtot' + Stb9) were selfed and constitute the 'Courtot' NILs.

383 **Pathogenicity assays**

384 Pathogenicity assays were performed following the procedure described by [18]. Briefly, 16 days old
385 plants were marked to delimit a 75 mm segment on the first true leaf. The segment was inoculated with
386 a paintbrush dipped into a 10^6 spores.mL^{-1} inoculum solution with one drop of Tween®20 added per 15
387 mL. After inoculation, the plants were watered and covered with transparent polyethylene bags for 72
388 hours to initiate the infection. The plants were kept in a climate chamber with a 16 h photoperiod (300
389 µmol.m^{-2}.s^{-1}), 80-90% relative humidity and 18°C night/22°C day. Phenotyping of the fungal population
390 was performed by visually assessing strain virulence on the cultivar 'Soissons' at 21 days post
391 inoculation (dpi). Visual assessments were made of percent of leaf area covered by necrosis (PLACN)
392 and by pycnidia (PLACP) within the inoculated segment of each leaf. Each of the 103 strains was tested
393 in three replicates with three leaves per replicate. Phenotyping of *AvrStb9* mutant strains was performed
394 following the same procedure.

395 For the host mapping populations, the Beaver/Soissons DH lines were inoculated with the strain
396 IPO09593, and the 220 wheat varieties were inoculated with the strains IPO09593 and IPO323. Here,
397 each interaction was tested in two replicates with three leaves per replicate and visual assessments of
398 PLACN and PLACP were recorded at 14, 20 and 26 dpi. We calculated the area under disease progress
399 curve for necrosis (AUDPCn) and sporulation (AUDPCs) with the formula:

400 $$\mathrm{AUDPC} = \frac{\sum[(t_{i+1} - t_i) \times (y_i + y_{i+1})]}{2}$$

401 With, $t_{i+1}-t_i$: number of days between two observations; y_i: PLACN or PLACP at day i; y_{i+1}: PLACN or
402 PLACP at day i+1. AUDPC were calculated relative to their maximum theoretical value, RAUDPCn
403 and RAUDPCs respectively. For all assays, disease severity data were averaged between replicates and
404 used as the input phenotype in GWAS and QTL analyses.

405 **Fungal whole-genome sequencing and variant calling**

406 Fungal spores were obtained after 7 days growth in liquid cultures of yeast extract-peptone-dextrose
407 Broth (Difco™ YPD Broth), and then freezed-dried during 24 h. High molecular weight DNA was
408 extracted using a phenol-chloroform based procedure. Illumina paired-end libraries were prepared for
409 each sample and DNA fragments sequenced with 2x100 bp reads on a HiSeq-2000 sequencing system
410 at Genewiz, Inc. (formerly Beckman Coulter Genomics). Depth of sequence coverage was variable
411 depending on the isolate, ranging from 16 to 303 genome equivalents with an average of 61 genome
412 equivalents. For each strain, reads were trimmed using trimmomatic v0.32 [45] and then mapped on the
413 reference genome IPO323 [42] using the mem algorithm from BWA v0.7.7 [46] with default options.
414 Samtools v0.1.19 and Picard tools v1.106 [47] were used to filter reads (optic duplicates, secondary
415 alignments and reads with a mapping quality < 30) and keep only pairs in which both reads met quality
416 checks. SNP calling was done with Freebayes v0.9 with the option --report-monomorphic [48]. All
417 positions detected as low-complexity regions or transposable elements (TE) were excluded using
418 RepeatMasker 4.0 with default options and REPET [49], respectively. Quality filters were applied on
419 the gVCF using in-house scripts. Depth of coverage (DP) calculated at each position follows a normal
420 distribution around the depth main peak; a DP filter was set at twice the standard deviation from the
421 mean. All the gVCF were stored into a matrix reduced to keep only the positions where at least one
422 strain has a detected SNP in a non-filtered position. The SNP matrix was parsed in .tped format,
423 converted to .ped/.map and filtered for < 0.5 missing data and > 0.1 minor allele frequency (MAF) using
424 PLINK v.1.9 [50].

425 **GWAS analyses**

426 For Genome-Wide Association Analysis (GWAS), we used the linear mixed model implemented in the
427 R package 'GAPIT' [51]. To account for population structure and reduce spurious associations, a kinship
428 matrix using the VanRaden method and the first three principal components computed from SNP data
429 were included a covariate in the model. We used a Bonferroni threshold of $p < 2.67e\text{-}7$ (α=0.05) to
430 declare significant SNPs associated with phenotypic variations. Linkage Disequilibrium (LD) measures
431 (r^2) for the significant SNPs were obtained with PLINK v.1.9 using the --r2 command and LD blocks
432 were visualized using the R package 'LDheatmap'. SNPs with an $r^2 \geq 0.5$ were considered in strong LD.

433 **Genetic mapping of *Stb9***

434 A genetic linkage map was available for the Beaver/Soissons DH population and contains 312
435 polymorphic loci: 121 SSR, 49 AFLP, 135 DArT markers and 7 major genes [43]. The map covers 1,526
436 cM with an average density of one marker per 12.6 cM. QTL mapping was conducted using RAUDPCs
437 and RAUDPCn phenotypes obtained from the isolate IPO09593 (*AvrStb9*) with R/qtl software v.1.48-1
438 [52]. Linkage analysis was performed for each trait with an initial Simple Interval Mapping (SIM),
439 followed by a Composite Interval Mapping (CIM). For SIM, 1000 genome-wide permutations were used
440 to calculate the significant logarithm of odds (LOD) threshold. Only QTLs that showed *p*-values less

441 than 0.05 were considered significant. Association mapping in the BW panel was done following the
442 exact same procedure as in the fungal population (see GWAS analyses). The 220 BW varieties have
443 been previously genotyped on an Affymetrix Axiom 410K single nucleotide polymorphism (SNP) array
444 [53]. Procedure of allele calling, filtering and quality check of genotype data are described in Balfourier
445 *et al.* [54]. For GWAS analysis, we excluded markers with less than 5% minor allele frequency and
446 more than 10% missing data and kept a set of 186,961 SNPs that passed quality control criteria and
447 could be anchored on the IWGSC annotation v2.1 [55]. We used filtered SNP data and phenotypes
448 (RAUDPCs and RAUDPCn) from the isolates IPO323 (*avrStb9*) and IPO09593 (*AvrStb9*) to perform
449 marker-trait associations.

450 **Gene annotation and expression analysis**

451 Predicted genes in the candidate region were retrieved from the *Z. tritici* reference genome annotation
452 [56]. We used RNA-seq data [20] mapping onto the reference genome IPO323 to manually curate
453 *Zt_1_693* (*AvrStb9)* gene model. Canonical and non-canonical splicing sites were confirmed by *de-novo*
454 transcriptome assembly obtained with DRAP [57]. The final gene model differed from those from
455 previous annotations due to errors in predicting correctly introns and includes two missing exons.
456 Candidate genes were screened for the presence of a secretion signal using SignalP 3.0 server [58].
457 Blastp was used to search for *AvrStb9* orthologous and paralogous proteins against the reference strain
458 IPO323 and closely-related *Zymoseptoria* species. Protein domains were searched using Interproscan
459 and structure homology prediction was performed in the HHpred server;
460 <https://toolkit.tuebingen.mpg.de/tools/hhpred>. For gene expression analysis, RNA-seq data samples
461 from *in vitro* and *in planta* (1, 4, 9, 14 and 21 dpi) conditions were obtained from Rudd *et al.* [20], and
462 gene expression quantified as fragments per kilobase of exon per million fragments mapped (FPKM)
463 using Cuffdiff v.2.2.1 [59]. *AvrStb9* DNA sequences are deposited in NCBI Genbank (accession
464 numbers OP376566 and OP376567).

465 **Construction of disruption plasmids**

466 For *AvrStb9* disruption, the hygromycin resistance marker (*hph*) was cloned between the 1,000 bp up-
467 and downstream flanking regions of the ORF, respectively. The following DNA fragments were
468 generated and cloned into pCAMBIA0380 plasmids (GenBank: AF234290.1). The up- and downstream
469 flanks were obtained by PCR on gDNA of IPO323 with primer pairs 1&2 and 5&6 (Table S2)
470 respectively using Q5 Hot Start High fidelity DNA polymerase (NEB, Evry, France). The *hph* was
471 amplified from pCAMBIA0380 with the primers 3 and 4 (Table S2). pCAMBIA0380 was digested by
472 *Eco*RI and *Xho*I and used for the cloning of three PCR fragments with Gibson Assembly cloning kit
473 (NEB, Evry, France) according to the supplier's indications. The ligation product was introduced into
474 NEB 5α competent *Escherichia coli* cells (NEB, Evry, France), transformants selected on kanamycin
475 (50 $\mu g.mL^{-1}$) containing LB-broth. Colonies were screened by PCR with the primer-pairs used for
476 cloning. Four positive colonies were chosen for plasmid extraction (Macherey & Nagel, Düren,

477 Germany) and restriction analysis. The construct was then introduced by electroporation into the
478 *Agrobacterium tumefaciens* Agl1 strain. Transformants were selected and isolated on YEB (5 g. L^{-1} beef
479 extract, 1 g. L^{-1} yeast extract, 5 g. L^{-1} peptone, 5 g. L^{-1} sucrose, 0.5 g. L^{-1} MgCl2, 1.5% agar) with
480 kanamycin (50 µg. mL^{-1}).

481 **Gene replacement constructs**

482 To swap *AvrStb9* alleles between virulent (IPO323) and avirulent (IPO09593) strains, the following
483 replacement cassettes were constructed. The respective *AvrStb9* alleles were amplified with primers 11
484 and 12 (Table S2) from IPO323 or IPO09593 gDNA. These fragments cover the ORF with 1 kb
485 upstream of the START codon and 360 bp downstream of the STOP codon. The *hph* (amplified with
486 primers 9 and 10 from pCAMBIA0380 plasmid DNA) and the 1 kb upstream flank of *AvrStb9* gene
487 (amplified with primers 7 and 8) were ligated to *AvrStb9* alleles into the *EcoRI-XhoI* digested
488 pCAMBIA0380, with Gibson Assembly cloning kit (NEB, Evry, France). Plasmids were introduced
489 into NEB 5α competent *E. coli* cells (NEB, Evry, France) and transformants selected on kanamycine
490 (50 µg.mL^{-1}) containing LB-broth. Colonies were screened by PCR with the primer-pairs used for
491 cloning. Four positive colonies were chosen for plasmid extraction (Macherey & Nagel, Düren,
492 Germany) and sequence analysis. These constructs named respectively pR323 and pR9593 were then
493 introduced by electroporation into the *Agrobacterium tumefaciens* Agl1 strain. Transformants were
494 selected and isolated on YEB with kanamycin (50 µg.mL^{-1}).

495 **Generation of *Z. tritici* transformants**

496 The transformation procedure was adapted from Zwiers & de Waard [60] and was performed as
497 previously described [61]. For *AvrStb9* deletion, the following *Z. tritici* strains were transformed with
498 the disruption plasmid: IPO323, IPO09593, IPO09359, IPO09139 and SYN32. Transformants were
499 selected and isolated twice on hygromycin (100 µg. mL^{-1}) containing medium. The replacement of the
500 *AvrStb9* ORF by the *hph* gene was checked by PCR on gDNA with the primer pair 13 and 14. The gene
501 deletion is expected to give a 1.6 kb fragment instead of the native 2.4 kb amplicon. The total number
502 of isolated and analyzed transformants were: IPO323 (n=144), IPO09593 (n=23), IPO09359 (n=26),
503 IPO09139 (n=46), SYN32 (n=38). One single transformant produced the expected PCR profile, namely
504 SYN32_ΔT12.

505 For *AvrStb9* allele swaps, IPO323 was transformed with plasmids pR323 and pR9593. Transformants
506 selected and isolated twice on hygromycin containing medium (100 µg. mL^{-1}). The replacement of
507 *AvrStb9* alleles in the transformants was checked by PCR using primers 15 and 16, leading to a single
508 1.6 kb amplicon in replacement mutants and to an additional 238 bp amplicon in ectopic transformants.
509 Transformants with the expected single band size were PCR checked with primers 17 and 18 as these
510 primers allow to distinguish the deletion of the amino acid residues 66-71 in the IPO09593 background

511 from the IPO323 one, and subsequently submitted to sequence analysis with primers indicated in Table
512 S2.

513 **Phylogenetic analysis.**

514 We used OrthoMCL algorithm to search for *AvrStb9* orthologous and paralogous protein sequences
515 using a cutoff E-value less than 1e-20 and filtering for low complexity regions [62];
516 <https://orthomcl.org/orthomcl/app/>. Of the 148 putative *AvrStb9* orthologs/paralogs identified
517 through OrthoMCL, we selected 122 by removing redundant information using the following criteria:
518 (*i*) when multiple identical sequences were present, one was arbitrarily chosen and retained; and (*ii*)
519 when multiple sequences from different strains of the same species were present, an arbitrarily chosen
520 strain (the reference strain, if known) was retained. A multiple sequence alignment was then generated
521 with Clustal Omega v1.2.4 [63] and alignment cleaning was performed using trimAL with the --
522 gappyout option [64]. We constructed a maximum likelihood tree of selected *AvrStb9* orthologs/paralogs
523 using RaxML with the GAMMA JTT model and 100 bootstrap replicates [65]. Phylogenetic trees were
524 visualized using iTOL [66]; <https://itol.embl.de/>.

525 **Population genetics and selection analyses**

526 In addition to the fungal population used for genetic analyses, we extended our sequence diversity and
527 selection analyses to include a global *Z. tritici* population originating from four distinct geographic
528 locations, including the middle East (n=30, Israel), Australia (n=27, Wagga Wagga), Europe (n=33,
529 Switzerland) and North America (n=56, Oregon, USA). Procedures of *de novo* genome assemblies and
530 sequence extraction were previously described [67]. We used DnaSP v6 [68] to calculate summary
531 statistics of the population genetic parameters associated with *AvrStb9*. Sliding window analyses of
532 nucleotide diversity (π) and Tajima's D were conducted in a window length of 200 bp and a step size of
533 20 bp. To test the selective pressure acting on *AvrStb9*, we estimated the rates of non-synonymous (dN)
534 and synonymous (dS) substitutions using CodeML from the PAML package [69]. A dN/dS (ω) ratio of
535 1 indicated neutrality, whereas $\omega < 1$ or > 1 suggested purifying or diversifying selection, respectively.
536 However, the presence of intragenic recombination could bias the ω rate testing. To account for these
537 issues, we performed the analysis with a non-recombining phylogenetic tree generated from the RDP4
538 software using RaxML with 100 bootstraps [70].

539

540 **Data Availability**

541 Genome sequencing data for the 103 French *Z. tritici* isolates is available at NCBI BioProject
542 PRJNA777581 (accessions SRR16762555 to SRR16762657). *AvrStb9* gene sequences are available at
543 NCBI Genbank (accession numbers OP376566 and OP376567).

544

Acknowledgements

We thank David Gouache, Henriette Goyeau, Gert H.J. Kema, Marc-Henri Lebrun, Frédéric Suffert and Anne-Sophie Walker for their contribution in establishing the fungal population; Johann Confais for his help in the virulence assays; Robert King and Jason Rudd for providing IPO323 RNA-seq data; Florence Cambon, the VégéPôle and GENTYANE platforms for the development of the Courtot NILs; Marc-Henri Lebrun for critical reading of the manuscript and valuable feedback; and Sophie Bouchet and Fanny Hartmann for assistance with the initial GWAS analyses. This work was supported by the French National Research Agency (program BIOADAPT, grant no. ANR-12-ADAP-0009-04), the French Fund to support Plant Breeding (FSOV 2008 H) and by BASF France SAS (V.I.S.A. project). INRAE BIOGER benefits from the support of Saclay Plant Sciences-SPS (ANR-17-EUR-0007).

Author contributions

T.C.M and S.F. conceived and designed the study. A.D. and S.G. performed virulence assays, C.A. performed the cloning and genetic transformations. S.O. provided DH seeds and linkage mapping data. C.S. provided the 'Courtot' NILs. J.C., N.L., J.A. and R.A performed bioinformatics analysis. D.C. provided sequence data from the global *Z. tritici* populations. R.A, T.C.M and S.F. analyzed the data and wrote the manuscript. All authors have reviewed the manuscript.

References

[1] Savary S, Willocquet L, Pethybridge SJ, Esker P, McRoberts N, Nelson A. The global burden of pathogens and pests on major food crops. Nat Ecol Evol. 2019; 3: 430–439.

[2] Lo Presti L, Lanver D, Schweizer G, Tanaka S, Liang L, Tollot M, *et al.* Fungal effectors and plant susceptibility. Annu Rev Plant Biol. 2015; 66: 513–545.

[3] Rocafort M, Fudal I, Mesarich CH. Apoplastic effector proteins of plant-associated fungi and oomycetes. Curr Opin Plant Biol. 2020; 56: 9-19.

[4] Jones JDG, Dangl JL. The plant immune system. Nature. 2006; 444: 323–329.

[5] Flor HH. The complementary genic systems in flax and flax rust**Joint contribution from the Field Crops Research Branch, Agricultural Research Service, United States Department of Agriculture and the North Dakota Agricultural Experiment Station. In: Demerec MBT-A in G, ed. Academic Press; 1956. pp. 29–54.

[6] Sánchez-Vallet A, Fouché S, Fudal I, Hartmann FE, Soyer JL, Tellier A, Croll D. The genome biology of effector gene evolution in filamentous plant pathogens. Annu Rev Phytopathol. 2018; 56: 21-40.

[7] Stergiopoulos I, de Wit PJGM. Fungal effector proteins. Annu Rev Phytopathol. 2009; 47: 233–263.

578 [8] Franceschetti M, Maqbool A, Jiménez-Dalmaroni MJ, Pennington HG, Kamoun S, Banfield MJ.
579 Effectors of filamentous plant pathogens: commonalities amid diversity. Microbiol Mol Biol Rev. 2017;
580 81: e00066–16.

581 [9] Petit-Houdenot Y, Lebrun MH, Scalliet G. Understanding plant-pathogen interactions in Septoria
582 tritici blotch infection of cereals. In: Achieving durable disease resistance in cereals. London, UK:
583 Burleigh Dodds Science Publishing; 2021. pp. 263-302.

584 [10] Battache M, Lebrun MH, Sakai K, Soudière O, Cambon F, Langin T, Saintenac C. Blocked at the
585 stomatal gate, a key step of wheat Stb16q-mediated resistance to *Zymoseptoria tritici*. Front Plant Sci.
586 2022; 13: 921074.

587 [11] Sánchez-Vallet A, McDonald MC, Solomon PS, McDonald BA. Is *Zymoseptoria tritici* a
588 hemibiotroph? Fungal Genet Biol. 2015; 79: 29–32.

589 [12] Fones H, Gurr S. The impact of Septoria tritici blotch disease on wheat: An EU perspective. Fungal
590 Genet Biol. 2015; 79: 3–7.

591 [13] Zhong Z, Marcel TC, Hartmann FE, Ma X, Plissonneau C, Zala M, *et al*. A small secreted protein in
592 *Zymoseptoria tritici* is responsible for avirulence on wheat cultivars carrying the *Stb6* resistance gene.
593 New Phytol. 2017; 214: 619–631.

594 [14] Kema GHJ, Mirzadi Gohari A, Aouini L, Gibriel HAY, Ware SB, van den Bosch F, *et al*. Stress and
595 sexual reproduction affect the dynamics of the wheat pathogen effector *AvrStb6* and strobilurin
596 resistance. Nature Genet. 2018; 50: 375–380.

597 [15] Meile L, Croll D, Brunner PC, Plissonneau C, Hartmann FE, McDonald BA, Sánchez-Vallet A. A fungal
598 avirulence factor encoded in a highly plastic genomic region triggers partial resistance to Septoria tritici
599 blotch. New Phytol. 2018; 219: 1048–1061.

600 [16] Brown JKM, Chartrain L, Lasserre-Zuber P, Saintenac C. Genetics of resistance to *Zymoseptoria*
601 *tritici* and applications to wheat breeding. Fungal Genet Biol. 2015; 79: 33–41.

602 [17] Yang N, McDonald MC, Solomon PS, Milgate AW. Genetic mapping of *Stb19*, a new resistance gene
603 to *Zymoseptoria tritici* in wheat. Theor Appl Genet. 2018; 131: 2765–2773.

604 [18] Langlands-Perry C, Cuenin M, Bergez C, Ben Krima S, Gélisse S, Sourdille P, *et al*. Resistance of the
605 wheat cultivar 'Renan' to Septoria leaf Blotch explained by a combination of strain specific and strain
606 non-specific QTL mapped on an ultra-dense genetic map. Genes. 2022; 13: 100.

607 [19] Suffert F, Sache I, Lannou C. Assessment of quantitative traits of aggressiveness in *Mycosphaerella*
608 *graminicola* on adult wheat plants. Plant Pathol. 2013; 62: 1330–1341.

609 [20] Rudd JJ, Kanyuka K, Hassani-Pak K, Derbyshire M, Andongabo A, Devonshire J, *et al*. Transcriptome
610 and metabolite profiling of the infection cycle of *Zymoseptoria tritici* on wheat reveals a biphasic
611 interaction with plant immunity involving differential pathogen chromosomal contributions and a
612 variation on the hemibiotrophic lifestyle definition. Plant Physiol. 2015; 167: 1158–1185.

613 [21] Chartrain L, Sourdille P, Bernard M, Brown JKM. Identification and location of *Stb9*, a gene for
614 resistance to Septoria tritici blotch in wheat cultivars Courtot and Tonic. Plant Pathol. 2009; 58: 547–
615 555.

616 [22] Huang Z, Feng Y, Chen D, Wu X, Huang S, Wang X, *et al*. Structural basis for activation and inhibition
617 of the secreted chlamydia protease CPAF. Cell Host Microbe. 2008; 4: 529-42.

618 [23] Palma-Guerrero J, Ma X, Torriani SFF, Zala M, Francisco CS, Hartmann FE, *et al*. Comparative
619 transcriptome analyses in *Zymoseptoria tritici* reveal significant differences in gene expression among
620 strains during plant infection. Mol Plant-Microbe Interact. 2017; 30: 231–244.

621 [24] Saintenac C, Lee W-S, Cambon F, Rudd JJ, King RC, Marande W, *et al*. Wheat receptor-kinase-like
622 protein *Stb6* controls gene-for-gene resistance to fungal pathogen *Zymoseptoria tritici*. Nature Genet.
623 2018; 50: 368–374.

624 [25] Saintenac C, Cambon F, Aouini L, Verstappen E, Ghaffary SMT, Poucet T, *et al*. A wheat cysteine-
625 rich receptor-like kinase confers broad-spectrum resistance against Septoria tritici blotch. Nat
626 Commun. 2021; 12: 433.

627 [26] Collemare J, Pianfetti M, Houlle A-E, Morin D, Camborde L, Gagey M-J, *et al. Magnaporthe grisea*
628 avirulence gene *ACE1* belongs to an infection-specific gene cluster involved in secondary metabolism.
629 New Phytol. 2008; 179: 196–208.

630 [27] Bourras S, McNally KE, Müller MC, Wicker T, Keller B. Avirulence genes in cereal powdery mildews:
631 the gene-for-gene hypothesis 2.0. Front Plant Sci. 2016; 7: 241.

632 [28] Hann DR, Gimenez-Ibanez S, Rathjen JP. Bacterial virulence effectors and their activities. Curr Opin
633 Plant Biol. 2010; 13: 388–393.

634 [29] López-Solanilla E, Bronstein PA, Schneider AR, Collmer A. HopPtoN is a *Pseudomonas syringae* Hrp
635 (type III secretion system) cysteine protease effector that suppresses pathogen-induced necrosis
636 associated with both compatible and incompatible plant interactions. Mol Microbiol. 2004; 54: 353–
637 365.

638 [30] Jashni MK, Mehrabi R, Collemare J, Mesarich CH, de Wit PJGM. The battle in the apoplast: Further
639 insights into the roles of proteases and their inhibitors in plant–pathogen interactions. Frontiers Plant
640 Sci. 2015; 6: 584.

641 [31] Chandrasekaran M, Thangavelu B, Chun SC, Sathiyabama M. Proteases from phytopathogenic
642 fungi and their importance in phytopathogenicity. J Gen Plant Pathol. 2016; 82: 233–239.

643 [32] Jashni MK, Dols IHM, Iida Y, Boeren S, Beenen HG, Mehrabi R, *et al*. Synergistic action of a
644 metalloprotease and a serine protease from *Fusarium oxysporum* f. sp. *lycopersici* cleaves chitin-
645 binding tomato chitinases, reduces their antifungal activity, and enhances fungal virulence. Mol Plant-
646 Microbe Interact. 2015; 28: 996–1008.

647 [33] Sanz-Martín JM, Pacheco-Arjona JR, Bello-Rico V, Vargas WA, Monod M, Díaz-Mínguez JM, *et al*.
648 A highly conserved metalloprotease effector enhances virulence in the maize anthracnose fungus
649 *Colletotrichum graminicola*. Mol Plant Pathol. 2016; 17: 1048–1062.

650 [34] Orbach MJ, Farrall L, Sweigard JA, Chumley FG, Valent B. A telomeric avirulence gene determines
651 efficacy for the rice blast resistance gene *Pi-ta*. Plant Cell. 2000; 12: 2019–2032.

652 [35] Khang CH, Park S-Y, Lee Y-H, Valent B, Kang S. Genome organization and evolution of the *AVR-Pita*
653 avirulence gene family in the *Magnaporthe grisea* species complex. Mol Plant-Microbe Interact. 2008;
654 21: 658–670.

655 [36] Irieda H, Inoue Y, Mori M, Yamada K, Oshikawa Y, Saitoh H, *et al*. Conserved fungal effector
656 suppresses PAMP-triggered immunity by targeting plant immune kinases. Proc Natl Acad Sci USA.
657 2019; 116: 496–505.

[37] Muszewska A, Stepniewska-Dziubinska MM, Steczkiewicz K, Pawlowska J, Dziedzic A, Ginalski K. Fungal lifestyle reflected in serine protease repertoire. Sci Rep. 2017; 7: 9147.

[38] Plummer KM, Clark SJ, Ellis LM, Loganathan A, Al-Samarrai TH, Rikkerink EHA, *et al*. Analysis of a secreted aspartic peptidase disruption mutant of *Glomerella cingulata*. Eur J Plant Pathol. 2004; 110: 265–274.

[39] ten Have A, Espino JJ, Dekkers E, van Sluyter SC, Brito N, Kay J, *et al*. The *Botrytis cinerea* aspartic proteinase family. Fungal Genet Biol. 2010; 47: 53–65.

[40] Gu Z, Steinmetz LM, Gu X, Scharfe C, Davis RW, Li W-H. Role of duplicate genes in genetic robustness against null mutations. Nature. 2003; 421: 63–66.

[41] Brunner PC, McDonald BA. Evolutionary analyses of the avirulence effector *AvrStb6* in global populations of *Zymoseptoria tritici* identify candidate amino acids involved in recognition. Mol Plant Pathol. 2018; 19: 1836–1846.

[42] Goodwin SB, Ben M'Barek S, Dhillon B, Wittenberg AHJ, Crane CF, Hane JK, *et al.* Finished genome of the fungal wheat pathogen *Mycosphaerella graminicola* reveals dispensome structure, chromosome plasticity, and stealth pathogenesis. PLoS Genet. 2011; 7: e1002070.

[43] Singh D, Simmonds J, Park RF, Bariana HS, Snape JW. Inheritance and QTL mapping of leaf rust resistance in the European winter wheat cultivar 'Beaver.' Euphytica. 2009; 169: 253–261.

[44] Touzy G, Rincent R, Bogard M, Lafarge S, Dubreuil P, Mini A, *et al.* Using environmental clustering to identify specific drought tolerance QTLs in bread wheat (*T. aestivum* L.). Theor Appl Genet. 2019; 132: 2859-2880.

[45] Bolger AM, Lohse M, Usadel B. Trimmomatic: a flexible trimmer for Illumina sequence data. Bioinformatics. 2014; 30: 2114–2120.

[46] Li H, Durbin R. Fast and accurate short read alignment with Burrows–Wheeler transform. Bioinformatics. 2009; 25: 1754–1760.

[47] Li H, Handsaker B, Wysoker A, Fennell T, Ruan J, Homer N, *et al*. The Sequence Alignment/Map format and SAMtools. Bioinformatics. 2009; 25: 2078–2079.

[48] Garrison E, Marth G. Haplotype-based variant detection from short-read sequencing. arXiv: 1207.3907v2. [Preprint]. 2012 [cited 2022 November 17]. Available from: https://doi.org/10.48550/arXiv.1207.3907

[49] Flutre T, Duprat E, Feuillet C, Quesneville H. Considering transposable element diversification in *de novo* annotation approaches. PLoS One. 2011; 6: e16526.

[50] Chang CC, Chow CC, Tellier LCAM, Vattikuti S, Purcell SM, Lee JJ. Second-generation PLINK: rising to the challenge of larger and richer datasets. GigaScience. 2015; 4: 7.

[51] Lipka AE, Tian F, Wang Q, Peiffer J, Li M, Bradbury PJ, *et al*. GAPIT: genome association and prediction integrated tool. Bioinformatics. 2012; 28: 2397–2399.

[52] Broman KW, Wu H, Sen Ś, Churchill GA. R/qtl: QTL mapping in experimental crosses. Bioinformatics. 2003; 19: 889–890.

[53] Danguy des Déserts A, Bouchet S, Sourdille P, Servin B. Evolution of recombination landscapes in diverging populations of bread wheat. Genome Biol Evol. 2021; 13: evab152.

697 [54] Balfourier F, Bouchet S, Robert S, De Oliveira R, Rimbert H, Kitt J, *et al.* Worldwide phylogeography
698 and history of wheat genetic diversity. Science Advances. 2022; 5: eaav0536.

699 [55] Zhu T, Wang L, Rimbert H, Rodriguez JC, Deal KR, de Oliveira R, *et al*. Optical maps refine the bread
700 wheat *Triticum aestivum* cv. Chinese Spring genome assembly. Plant J. 2021; 107: 303–314.

701 [56] Grandaubert J, Bhattacharyya A, Stukenbrock EH. RNA-seq-based gene annotation and
702 comparative genomics of four fungal grass pathogens in the genus Zymoseptoria identify novel orphan
703 genes and species-specific invasions of transposable elements. G3 Genes Genomes Genet. 2015; 5:
704 1323–1333.

705 [57] Cabau C, Escudié F, Djari A, Guiguen Y, Bobe J, Klopp C. Compacting and correcting Trinity and
706 Oases RNA-Seq de novo assemblies. PeerJ. 2017; 5: e2988.

707 [58] Dyrløv Bendtsen J, Nielsen H, von Heijne G, Brunak S. Improved prediction of signal peptides:
708 SignalP 3.0. J Mol Biol. 2004; 340: 783–795.

709 [59] Trapnell C, Roberts A, Goff L, Pertea G, Kim D, Kelley DR, *et al*. Differential gene and transcript
710 expression analysis of RNA-seq experiments with TopHat and Cufflinks. Nat Protoc. 2012; 7: 562–578.

711 [60] Zwiers L-H, de Waard MA. Efficient *Agrobacterium tumefaciens*-mediated gene disruption in the
712 phytopathogen *Mycosphaerella graminicola*. Curr Genet. 2001; 39: 388–393.

713 [61] Omrane S, Sghyer H, Audéon C, Lanen C, Duplaix C, Walker A-S, Fillinger S. Fungicide efflux and
714 the MgMFS1 transporter contribute to the multidrug resistance phenotype in *Zymoseptoria tritici* field
715 isolates. Environ Microbiol. 2015; 17: 2805–2823.

716 [62] Li L, Stoeckert Jr CJ, Roos DS. OrthoMCL: identification of ortholog groups for eukaryotic genomes.
717 Genome Res. 2003; 13: 2178–2189.

718 [63] Sievers F, Wilm A, Dineen D, Gibson TJ, Karplus K, Li W, *et al*. Fast, scalable generation of high-
719 quality protein multiple sequence alignments using Clustal Omega. Mol Syst Biol. 2011; 7: 539.

720 [64] Capella-Gutiérrez S, Silla-Martínez JM, Gabaldón T. trimAl: a tool for automated alignment
721 trimming in large-scale phylogenetic analyses. Bioinformatics. 2009; 25: 1972–1973.

722 [65] Stamatakis A. RAxML version 8: a tool for phylogenetic analysis and post-analysis of large
723 phylogenies. Bioinformatics. 2014; 30: 1312–1313.

724 [66] Letunic I, Bork P. Interactive tree of life (iTOL) v3: an online tool for the display and annotation of
725 phylogenetic and other trees. Nucleic Acids Res. 2016; 44: W242–W245.

726 [67] Hartmann FE, Sánchez-Vallet A, McDonald BA, Croll D. A fungal wheat pathogen evolved host
727 specialization by extensive chromosomal rearrangements. ISME J. 2017; 11: 1189–1204.

728 [68] Rozas J, Ferrer-Mata A, Sánchez-DelBarrio JC, Guirao-Rico S, Librado P, Ramos-Onsins SE, Sánchez-
729 Gracia A. DnaSP 6: DNA Sequence Polymorphism analysis of large data sets. Mol Biol Evol. 2017; 34:
730 3299–3302.

731 [69] Nielsen R, Yang Z. Likelihood models for detecting positively selected amino acid sites and
732 applications to the HIV-1 envelope gene. Genetics. 1998; 148: 929–936.

733 [70] Martin DP, Murrell B, Golden M, Khoosal A, Muhire B. RDP4: Detection and analysis of
734 recombination patterns in virus genomes. Virus Evol. 2015; 1.

735

736 ## Figures captions

737

738 **Figure 1.** GWAS identifies a candidate gene controlling avirulence on the cultivar 'Soissons'. (a) Manhattan plot
739 representing the association of multiple SNPs with PLACN on cultivar 'Soissons'. The X and Y axes indicate
740 positions on chromosome 1 and −log10 (*p*-value) for associations, while the red line represents the Bonferroni
741 threshold (α=0.05). (b) Top: Gene annotations (black arrows) and transposable elements (grey arrow) on the
742 reference genome IPO323. The candidate gene is highlighted in red. Bottom: Pairwise linkage disequilibrium plot
743 around the lead significant SNP. The association peak is associated with several polymorphisms in the gene
744 *Zt_1_693*. (c) The difference in PLACN of isolates carrying the virulent and avirulent alleles (based on the lead
745 SNP). Significance difference from the mean was computed using a two-sided Mann-Whitney test (****,
746 $p<0.0001$). (d) Gene expression profile of *Zt_1_693* measured as fragments per kilobase of exon per million
747 mapped fragments (FPKM) throughout the time course of *Z. tritici* infection on a susceptible wheat cultivar [20].

748 **Figure 2.** *Zt_1_693* encodes for the avirulence gene *AvrStb9* and triggers *Stb9* resistance. (a) PLACP at 26 dpi
749 measured after inoculation with the avirulent isolate IPO09593, the virulent isolate IPO323 and IPO323 mutants
750 expressing the avirulent allele ($IPO323_{Avrstb9}$) or the virulent allele ($IPO323_{avrstb9}$) on cultivars 'Courtot' (*Stb9*), a
751 'Courtot' mutant lacking *Stb9* and 'Soissons' (details on the phenotype of each mutant is provided in Fig. S6;
752 Table S6). Statistical significance was determined using a Tukey's HSD test. (b) Genetic mapping of *Stb9*
753 resistance gene using linkage mapping. Top panel: Linkage map and marker position in cM. Bottom panel:
754 Logarithm of odds (LOD) score plot of the QTL analysis (Relative AUDPC for sporulation and necrosis in black
755 and grey, respectively) possibly containing the *Stb9* locus mapped to the long arm of the chromosome 2B. The
756 horizontal dashed line indicates a suggestive linkage threshold (LOD = 3). The position of the marker in the QTL
757 peak is highlighted in red. (c) Manhattan plots representing association mapping results of relative AUDPC
758 sporulation of the avirulent (top) and virulent (bottom) isolates in the bread wheat panel. Multiple SNPs in the
759 telomeric region of chromosome 2B associated with the avirulent isolate are located in the *Stb9* genomic region.

760 **Figure 3.** *AvrStb9* diversity and phylogeny in the global *Z. tritici* population. (a) The top panel shows the *AvrStb9*
761 gene structure. Middle and low panels are sliding window analyses for nucleotide diversity (π) and Tajima's D
762 across the *AvrStb9* locus, respectively, with a window size of 200 bp and a step size of 20 bp. The plots show a
763 reduced nucleotide diversity and a drop in Tajima's D values, likely corresponding to a selective sweep spanning
764 the region. (b) Schematic diagram of *AvrStb9* protein sequence with an annotation of amino acid substitutions
765 between virulent and avirulent alleles. Substitutions potentially involved in virulence are highlighted in red.
766 SP=Signal peptide. (c) A phylogenetic tree of *AvrStb9* protein sequence generated from a global *Z.*
767 *tritici* population and the reference isolate IPO323.

768 **Figure 4.** Phylogenetic tree of selected *AvrStb9* orthologs/paralogs belonging to five distinct classes of
769 Ascomycota lineages. Leaf labels are color-coded according to class and represent abbreviated names of the fungal
770 species (Table S4). *AvrStb9* is indicated with a black arrow.

771

772 **Supporting information captions**

773

774 **Table S1.** Summary statistics of GWA analysis on Stb9 resistance in the BW panel.

775 **Table S2.** List of primers used in this study.

776 **Table S3.** Mean PLACP (%) measured among wild-types, mutant and chimeric strains of Avrstb9
777 alleles.

778 **Table S4.** List of AvrStb9 selected homologs identified by blastP search against UniProtKB and NCBI
779 database.

780 **Table S5.** Model test and parameter estimates of diversifying selection with codeml.

781

782 **Figure S1.** Density distribution of percentage of leaf area covered by pycnidia (PLACP) in the fungal
783 population.

784 **Figure S2.** Population structure and relatedness in the fungal population used for GWAS analysis.

785 **Figure S3.** Manhattan plots of PLACN and PLACP on the wheat cultivar 'Soissons'.

786 **Figure S4.** Improved *Avrstb9* gene model using RNA-seq reads mapped to the reference genome
787 IPO323.

788 **Figure S5.** Distribution of the relative AUDPC sporulating leaf area in the breed wheat population and
789 lead GWAS SNP phenotypes.

790 **Figure S6.** Wild-type, mutant and chimeric strains phenotype (PLACP) on cultivars carrying or not the
791 resistance gene *Stb9* and the susceptible cultivar Taichung-29.

792 **Figure S7.** *AvrStb9* paralogs and their expression profile.

793